

Synthesis, characterization, and thermally activated polymerization behavior of bisphenol-S/aniline based benzoxazine

Yanfang Liu*, Zaiqin Yue, Jungang Gao

College of Chemistry and Environmental Science, Hebei University, Baoding 071002, China

ARTICLE INFO

Article history:

Received 24 February 2010

Received in revised form

25 May 2010

Accepted 2 June 2010

Available online 9 June 2010

Keywords:

Benzoxazine

Bisphenol-S

Ring-opening polymerization

ABSTRACT

A difunctional benzoxazine monomer, 6,6'-bis(3-phenyl-3,4-dihydro-2H-benzo[e][1,3]oxazinyl) sulfone (BS-a), was synthesized via a solution method from bisphenol-S, aniline and formaldehyde. The chemical structure of the benzoxazine was confirmed by ^1H and ^{13}C nuclear magnetic resonance spectroscopy, Fourier transform infrared (FTIR) spectroscopy, elemental analysis, and size exclusion chromatography. The ring-opening polymerization of BS-a monomer was investigated with FTIR under air and nitrogen atmospheres, and with differential scanning calorimetry (DSC) in both dynamic and isothermal conditions. The FTIR results show that the absorption intensities of C–O–C, C–N–C, and oxazine ring decrease gradually with temperature and time rising during the polymerization reaction. The change rates of some absorption intensities of oxazine ring are affected by different atmospheric environments, and a higher degree of conversion is obtained in nitrogen than that in air at the same reaction temperature and in equal time. Kinetic parameters of the dynamic polymerization DSC results were evaluated with Kissinger and Ozawa methods, respectively. The isothermal DSC results show that the polymerization reaction of BS-a monomer follows an autocatalytic mechanism.

© 2010 Elsevier Ltd. All rights reserved.

1. Introduction

Benzoxazine is a newly developed thermosetting phenolic resin, and it can be synthesized via Mannich condensation from phenol, amine and formaldehyde [1,2]. Various phenols and amines offer enormous flexibility in molecular-design for benzoxazine, and a few number of benzoxazine monomers with different structures have been synthesized [3–10]. The benzoxazine monomer can be polymerized by a thermally activated ring-opening polymerization reaction with no reaction byproducts released and no catalyst required [10–16]. During the self-crosslinking polymerization reaction, the Mannich bridge structure ($-\text{CH}_2-\text{NR}-\text{CH}_2-$) was formed between benzoxazine molecules through the ring-opening reaction of oxazine rings. So, with the polymerization proceeding, benzoxazine gradually convert into a three-dimension network of polybenzoxazine. The benzoxazine-based materials possess excellent mechanical and thermal properties, high dimensional stability, low water absorption, and high char yield, which make benzoxazine a promising matrices candidate for high performance

composites, especially in microelectronics, aerospace and packaging industry [15–17].

The properties of the polybenzoxazine materials depend on benzoxazine monomer molecular structure and the polymerization processing conditions, and it is essential to understand the polymerization behavior of different benzoxazine resins to define the actual processing conditions. In recent years, the majority of studies were reported on synthesis methods [3,18], polymerization [19–22], blending and composites [23–28], modification [16,29–31], properties [32–34], and degradation [35] of benzoxazine monomers and the resultant polymers. Most research articles were concerned with the studies of the popular bisphenol-A based difunctional benzoxazine, while the bisphenol-S based benzoxazine was seldom studied [5,12]. Different from the isopropyl in bisphenol-A, the sulfone ($-\text{SO}_2-$) moiety in bisphenol-S is a strong electron-withdrawing group with high rigidity. Introducing sulfone moiety into benzoxazine can enhance its rigidity and improve its thermal stability. In the literatures, sulfone-based benzoxazine was briefly mentioned as part of many compound study [5], and synthesis and structure prediction of benzoxazine based on bisphenol-S and methylamine was reported [12].

The objective of this paper is to perform a comprehensive study for the polymerization reaction of a benzoxazine monomer based on bisphenol-S and aniline, and to understand the polymerization

* Corresponding author. Fax: +86 312 5079525.

E-mail address: liuyanfang@msn.com (Y. Liu).

behavior and reaction mechanism of the benzoxazine. In the paper, the difunctional benzoxazine monomer, 6,6'-bis(3-phenyl-3,4-dihydro-2H-benzo[e][1,3]oxaziny) sulfone (abbreviated as BS-a), was synthesized via a solution method from bisphenol-S, aniline and formaldehyde. The ring-opening polymerization of BS-a monomer was investigated with Fourier transform infrared (FTIR) spectroscopy in both air and nitrogen atmospheres, and with differential scanning calorimetry (DSC) in both dynamic and isothermal conditions.

2. Experimental

2.1. Materials

Bisphenol-S (4,4'-dihydroxydiphenyl sulfone) (99%), was purchased from Shanghai Chemical Reagent Co. (China). Formaldehyde (37% aqueous), aniline, dioxane and chloroform were obtained from Tianjin Chemical Reagent Co. (China). All chemicals were used as received.

2.2. Synthesis of 6,6'-bis(3-phenyl-3,4-dihydro-2H-benzo[e][1,3]oxaziny) sulfone

To a 100 mL three-necked round bottom flask equipped with a mechanical stirrer, a thermometer, and a reflux condenser, 4.5 mL aniline, 8.1 g formaldehyde, and 20 mL dioxane were added, keeping the temperature below 10 °C in an ice bath. The mixture was stirred for 15 min before adding the solution of 6.26 g bisphenol-S in 15 mL dioxane. The temperature was then gradually raised to 92 °C, and the mixture was allowed to reflux for 6 h. Subsequently, the solvent was removed by distillation under reduced pressure, and the residue was dissolved in 20 mL chloroform. The chloroform solution was washed several times with 3 mol L⁻¹ NaOH aqueous solution and de-ionized water, respectively. During the purification process, the product was precipitated and filtered out in a separatory funnel. Thereafter, it was dried at 60 °C in a vacuum oven for 7 h and then at 70 °C in an air circulated oven for 8 h, and a pale yellow powder was obtained.

2.3. Measurements

Both proton (¹H) and carbon (¹³C) nuclear magnetic resonance (NMR) spectra were recorded using a Bruker Avance 600 NMR spectrometer at a proton frequency of 600 MHz and the corresponding carbon frequency. Deuterated acetone was used as a solvent and tetramethylsilane as an internal standard.

FTIR spectra were obtained with a Nicolet 380 FTIR spectrometer at a resolution of 4 cm⁻¹. BS-a sample was finely ground with KBr powder and pressed into disk. For polymerization study, the BS-a monomer in KBr disk was isothermally polymerized in an oven under either circulating air or nitrogen atmosphere. During the polymerization reaction, the disk was repeatedly withdrawn at a regular time interval for measurement.

The quantitative analyses of C, H, N, O and S were carried out on an Exeter Analytical CE-440 elemental analyzer.

Size exclusion chromatography (SEC) was performed on a Waters workstation equipped with a 515 HPLC pump, a 717 auto sample injector and a 2410 refractive index detector. Three styragel columns (HT3, HT5, and HT6E, with pore sizes of 100 nm, 10,000 nm, and 100,000 nm, respectively) were connected in series. The measurements were performed at a column temperature of 25 °C with tetrahydrofuran as an eluent and at a flow rate of 1.0 mL/min. The concentration of BS-a was 2 mg/mL in tetrahydrofuran, and the injecting amount for measurement was 50 μL.

The dynamic and isothermal polymerization reactions of BS-a monomer were monitored with a Shimadzu DSC-41 differential scanning calorimeter operating in a nitrogen atmosphere. The DSC instrument was calibrated with high purity indium. α-Al₂O₃ was used as the reference material. The amount of BS-a used was about 6.5 mg. In the dynamic analyses, the samples were scanned at different heating rates of 5, 7.5, 10, 12.5, and 15 °C/min, respectively. Isothermal analyses were performed at temperatures of 172, 176, 182, 187, 191, and 197 °C, respectively. Before loading the sample, the furnace was first heated up to a desired temperature and kept for a certain period of time. When the system reached an equilibrium state, the sample cell was quickly set on the calorimetric detector plate. The reaction was considered complete when the rate curve leveled off to a baseline. After each isothermal run, the sample was rapidly cooled to 10 °C and then reheated at 10 °C/min to 280 °C to determine the residual heat of reaction, ΔH_r. Therefore, the total heat evolved during the polymerization reaction is ΔH₀ = ΔH_i + ΔH_r.

3. Results and discussion

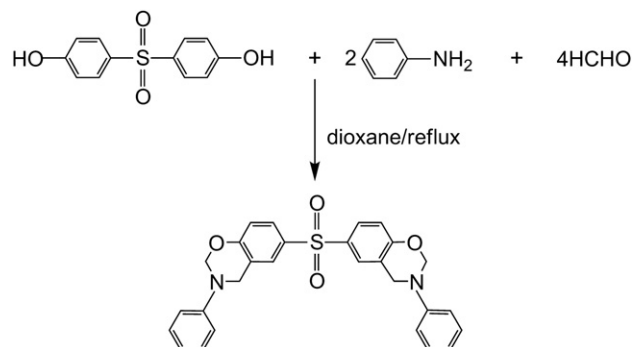
3.1. Synthesis and characterization

BS-a was synthesized via a solution method [2], and the synthesis reaction mechanism is shown in Scheme 1. The chemical structure of BS-a was confirmed with ¹H and ¹³C NMR, FTIR, element analysis, and SEC.

Fig. 1 shows the ¹H NMR spectrum of BS-a. Resonances appearing at 4.75 ppm and 5.52 ppm are assigned to the methylene protons of Ar-CH₂-N and O-CH₂-N of the oxazine ring, respectively. The multiplets at 6.79–6.89, 7.08–7.22, 7.63–7.72 ppm are assigned to the aromatic protons.

In the corresponding ¹³C NMR spectrum in Fig. 2, resonances appearing at 50.3 ppm and 80.7 ppm are assigned to the methylene carbons (C5 and C6) of Ar-CH₂-N and O-CH₂-N of the oxazine ring, respectively. Other chemical shifts (ppm) are assigned to the aromatic carbon resonances: 118.2 (C3), 118.9 (C8), 122.2 (C1), 123.1 (C11), 127.8 (C12), 128.3 (C9), 129.8 (C2), 130.0 (C2), 135.0 (C10), 148.7 (C4), 159.2 (C7).

The FTIR spectrum of BS-a is shown in Fig. 3A. The characteristic absorptions at 1078, 1118 and 1194 cm⁻¹ are assigned to the asymmetric stretching of C-N-C, while the absorption peak at 792 cm⁻¹ is assigned to the symmetric stretching of C-N-C [36]. The characteristic absorptions at 1030 and 1238 cm⁻¹ are due to the symmetric and asymmetric stretching of C-O-C [36], respectively. The peak at 1329 cm⁻¹ is due to CH₂ wagging mode in benzoxazine structure [15–17]. The absorption at 971 cm⁻¹ is attributed to the benzene with an attached oxazine ring [37], and the peaks at 722 and 664 cm⁻¹ are due to the absorptions of oxazine ring. In addition, the absorption at 1600 cm⁻¹ is assigned to C=C stretching of benzene ring. The absorptions at 1483 and 1493 cm⁻¹ are due to the



Scheme 1. Chemical reaction of BS-a monomer synthesis.

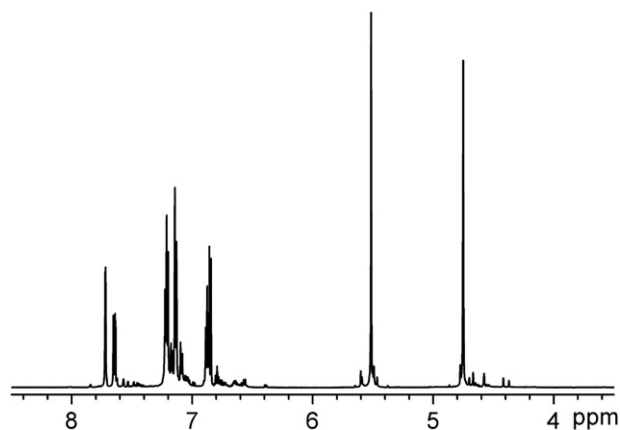


Fig. 1. ^1H NMR spectrum of BS-a monomer.

stretching vibrations of the benzene ring attached to oxazine ring, and the out-of-plane bending mode can be found at 919 cm^{-1} [38,39], while the in-plane bending mode is at 577 cm^{-1} [36]. Moreover, the peak at 825 cm^{-1} is assigned to C–H out-of-plane bending vibrations of 1,4-substituted benzene ring, and the absorption bands characteristic of C–H out-of-plane deformation vibration of meta-disubstituted benzene ring appeared at 693 and 756 cm^{-1} . Besides, C–H stretching vibrations of benzene ring appeared at 3020 cm^{-1} , and the peaks at 2923 and 2850 cm^{-1} are assigned to the asymmetric and symmetric stretching vibrations of CH_2 of oxazine ring, respectively. The absorption at 1097 cm^{-1} is due to the stretching vibrations of aromatic C–S, and the peaks at 1140 and 1297 cm^{-1} are assigned to the symmetric and asymmetric stretching vibrations of $\text{O}=\text{S}=\text{O}$ group, respectively.

Elemental analysis of BS-a shows that the experimental results (C, 68.67%; H, 5.05%; N, 6.25%; O, 13.43%; S, 6.58%) are in reasonable agreement with the calculated value (C, 69.40%; H, 4.99%; N, 5.78%; O, 13.21%; S, 6.62%).

The SEC chromatogram is shown in Fig. 4, and the weight-average molecular weight is 500. Comparing the SEC results with the calculated molecular weight value, 484.6, it can be deduced that no oligomeric fraction exists in the initial BS-a monomer, which is in good agreement with ^1H and ^{13}C NMR spectra, indicating that no protons or carbons exist from the methylene groups as a result of the ring-opening of oxazine ring.

3.2. Structure changes during the ring-opening polymerization reaction

Fig. 3B–D are the FTIR spectra of BS-a polymerized under air atmosphere at $170\text{ }^\circ\text{C}$ for different times. With the polymerization

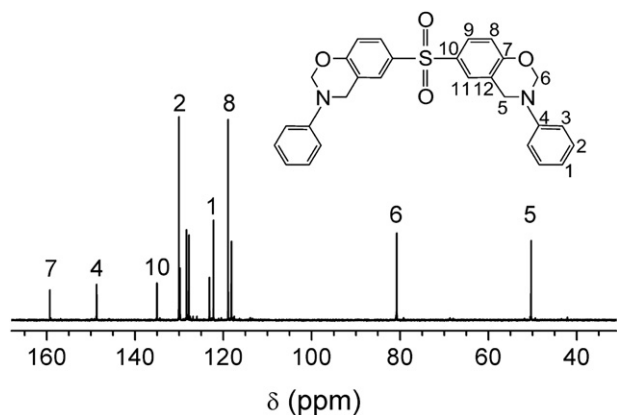


Fig. 2. ^{13}C NMR spectrum of BS-a monomer.

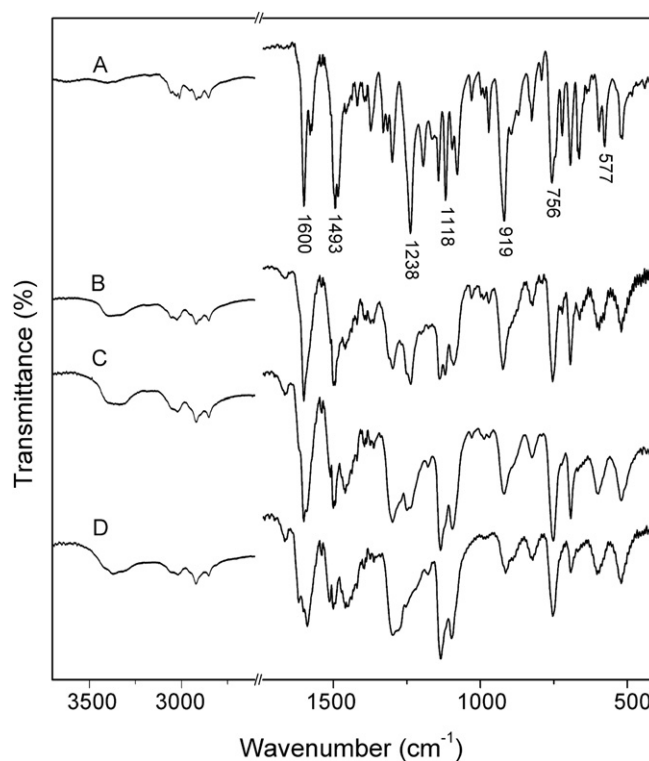


Fig. 3. FTIR spectra of: (A) BS-a monomer, and polymerized at $170\text{ }^\circ\text{C}$ in air for: (B) 30 min, (C) 60 min, and (D) 180 min.

reaction proceeding, chemical structure changes can be traced from the FTIR spectra. Some obvious changes are located at 1238 , 1194 , 1118 , 1078 , 1030 , 722 , 664 cm^{-1} , and the intensities of these bands decreased with the reaction time increasing, which are associated with the variations of the absorption intensities of C–O–C, C–N–C, and oxazine ring, owing to the ring-opening reaction of BS-a. Meanwhile, corresponding to the decrease of these absorption intensities, some new absorption bands appeared. Among these, the new band at $3350\text{--}3390\text{ cm}^{-1}$ is assigned to the stretching of OH group formed through oxazine ring-opening reaction, and the new absorption at 1650 cm^{-1} may be attributed to Schiff base, $\text{N}=\text{CH}$, a possible intermediate of oxazine ring-opening polymerization [20,38,40]. With reaction time rising, these new peaks became wider and their absorption intensities increased. Moreover, other obvious changes located at 1618 , 1600 , 1587 , 1512 , 1493 , 1483 , 1456 ,

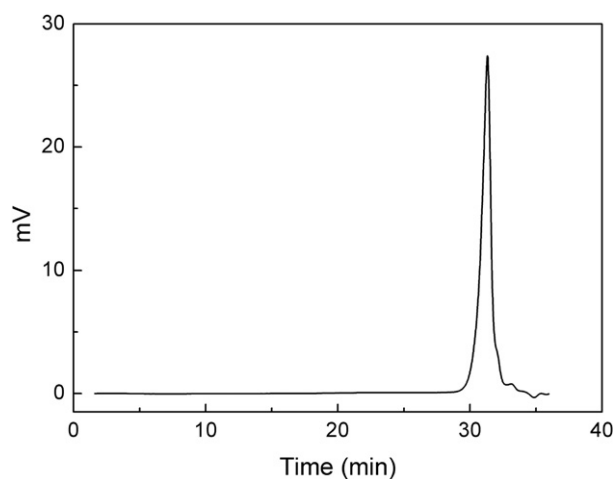


Fig. 4. SEC chromatogram of BS-a monomer.

1452, 971, 919, 825, 693, 577 cm^{-1} are the absorptions associated with benzene ring. Corresponding to the intensities decreasing of C–O–C, C–N–C, and oxazine ring, the absorption intensities at 1600, 1493, 1483, 919, 825, 693 cm^{-1} also reduced, while the intensities at 1618, 1587, 1512, 1456, 1452 cm^{-1} increased, which is attributed to the variation of the numbers of the substituted groups attached to benzene ring, namely tri-substituted benzene ring converts into tetra-substituted. According to the structure changes during BS-a polymerization, the ring-opening polymerization reaction can be described as in Scheme 2.

To evaluate the effect of the atmospheric environments on the polymerization reaction, the polymerization of BS-a in nitrogen atmosphere was also monitored by FTIR, and some FTIR spectra are shown in Fig. 5. Comparing the FTIR spectra with that in Fig. 3, some difference of absorption changes can be discerned.

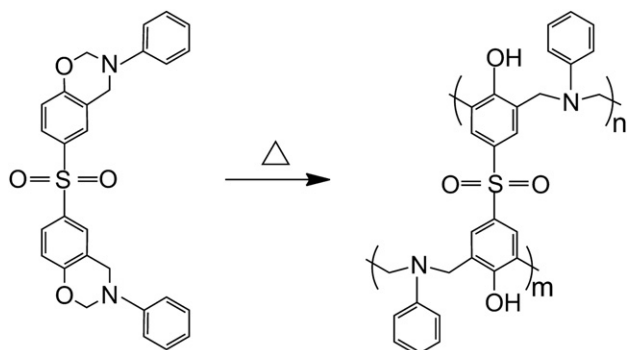
In order to analyze quantitatively the absorption intensity changes in the FTIR spectra, some absorptions were normalized and their relative conversions (α) at various isothermal polymerization temperatures were determined as follow [13,20,26]:

$$\alpha = 1 - \frac{(A_i/A_r)_{T,t}}{(A_i/A_r)_{T,t=0}} \quad (1)$$

where T is the polymerization temperature and t is the polymerization time, $(A_i/A_r)_{T,t}$ and $(A_i/A_r)_{T,t=0}$ are the ratios of integrated intensity of the specified band to the integrated intensity of the internal standard band at time t and at starting time, respectively. The band at 756 cm^{-1} is used as an internal standard.

According to equation (1), the conversions of different absorption bands were calculated in air and nitrogen at different temperatures for various times. And some plots of conversion against reaction time are shown in Fig. 6. It is apparent that polymerization environment (temperature and atmosphere) greatly affected the thermally activated polymerization process. On one hand, the effect of temperature is significant on the conversion change rates of various absorption bands in air and nitrogen. For a selected band, in the same reaction time, a higher conversion was gained at a higher reaction temperature. On the other hand, it is obvious that under air condition the polymerization proceeds slower than that in nitrogen, and the degree of changes in air for a selected band was lower than that in nitrogen at the same reaction temperature and in equal time, which may be ascribed to the decreased catalytic effect of phenolic hydroxyl groups partly oxidized in air.

Generally, the reaction is considered to be cationic polymerization, and the oxazine ring-opening is catalyzed by phenolic hydroxyl groups formed during the early stages of heating [19,41]. In BS-a monomer polymerization, the phenolic hydroxyl groups are liable to be oxidized in air due to the electronic effects of the



Scheme 2. Thermally activated ring-opening polymerization of BS-a monomer.

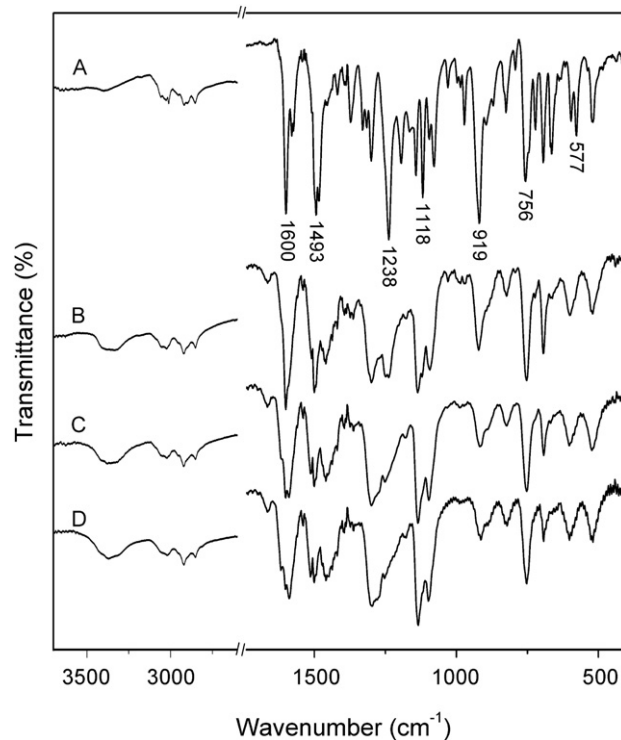


Fig. 5. FTIR spectra of: (A) BS-a monomer, and polymerized at 170 °C in nitrogen for: (B) 10 min, (C) 30 min, and (D) 60 min.

electron-withdrawing sulfone group ($-\text{SO}_2-$), which makes BS-a polymerization proceed slower in air than that in nitrogen. However, different reaction trends were earlier observed with FTIR and DSC in air and nitrogen in other type benzoxazines polymerization, respectively [20,38].

In addition, it would be observed that at the same reaction temperature the reaction rates of these selected bands were different, which can in some extent indicate the reaction sequence or activity for various chemical reaction sites during the polymerization. Among these selected bands, the intensity change rates of bands at 1238, 1118, 722 cm^{-1} are higher than those of other bands, and the change rate of band at 1030 cm^{-1} is the lowest.

3.3. Ring-opening polymerization kinetics

The polymerization kinetic analysis for thermosetting resins can be performed using several techniques based on different measurement principles, such as, DSC [19,42,43], FTIR [44], NMR [45], and rheology [22]. Among these techniques, DSC is based on a phenomenological method, with which kinetic analysis only need to calculate the heat variation for a whole reaction process with temperature or time, and not to distinguish individual reaction in the process. So DSC is the most utilized technique to determine kinetic parameters and rate equation of benzoxazine polymerization [19,28,46], and both dynamic and isothermal DSC modes can be used to characterize the polymerization process.

In this study, a multiple-heating-rate method for dynamic mode was used to evaluate the polymerization reaction kinetic parameters by measuring the exothermic peak temperatures (T_p s) at several heating rates. Fig. 7 shows the DSC curves of BS-a dynamic polymerization. During the heating process, an endothermic peak appeared at about 100 °C, which corresponds to the melting processes of BS-a. With the temperature rising, an exothermic reaction process covered a wide temperature range, which corresponds to the polymerization of BS-a. Based on the difference of the exothermic peak

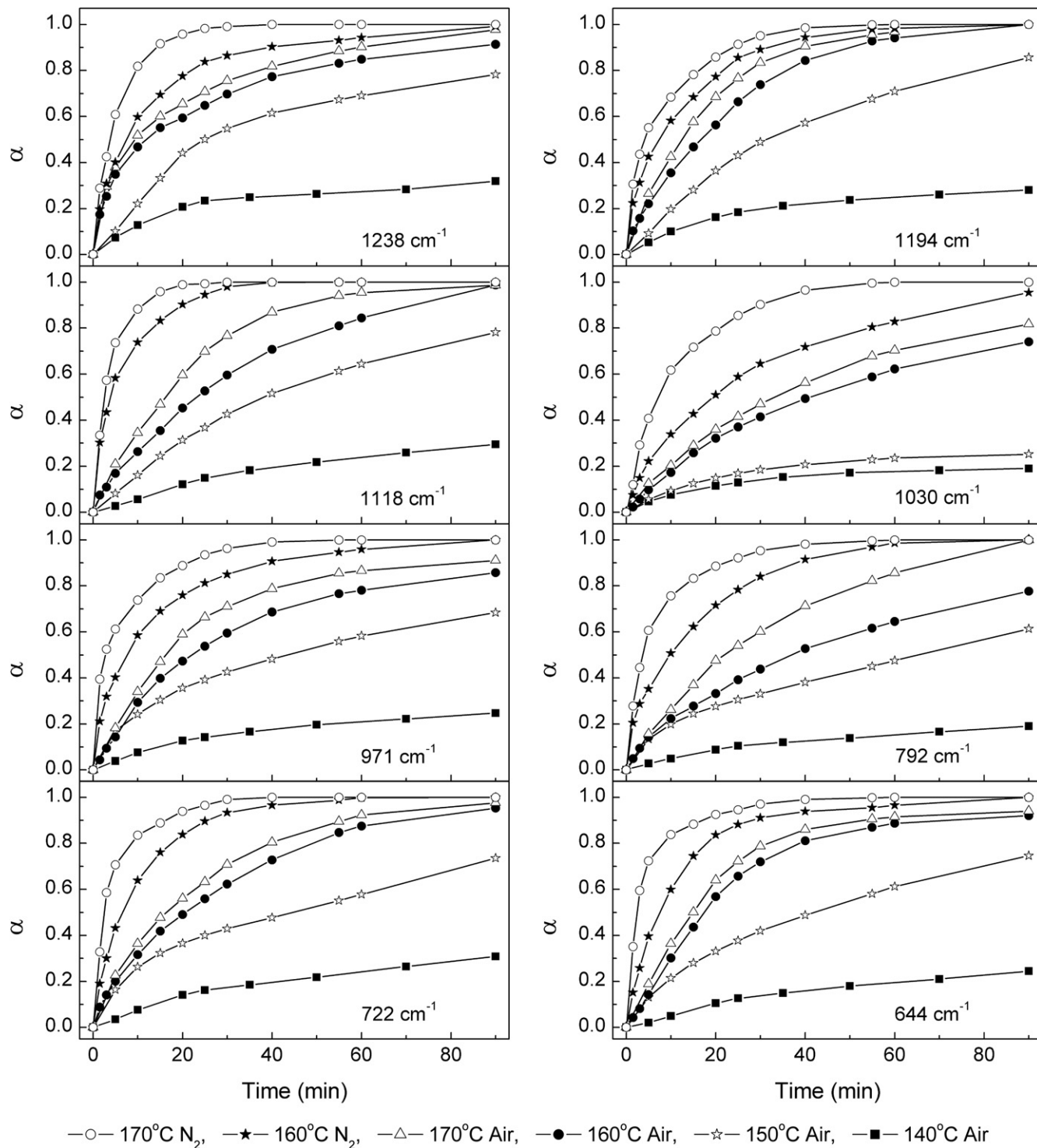


Fig. 6. Plots of conversion versus reaction time for different absorption bands at different temperatures in air and nitrogen.

temperatures of the DSC curves, the kinetic parameters can be determined by Kissinger and Flynn–Wall–Ozawa methods [47–49].

Kissinger's technique assumes that the maximum reaction rate occurs at peak temperatures, where $d^2\alpha/dt^2 = 0$, it can be expressed as

$$\ln\left(\frac{\beta}{T_p^2}\right) = \ln\left(\frac{AR}{E}\right) - \frac{E}{RT_p} \quad (2)$$

where β is the linear heating rate, A is the pre-exponential factor, E is the activation energy and R is the universal gas constant. Therefore, a plot of $\ln(\beta/T_p^2)$ versus $1/T_p$ gives the values of E and A .

Flynn–Wall–Ozawa method assumes that the degree of conversion at peak temperatures for different heating rates is constant, and it can be expressed as

$$\ln\beta = -1.052\frac{E}{RT} + C \quad (3)$$

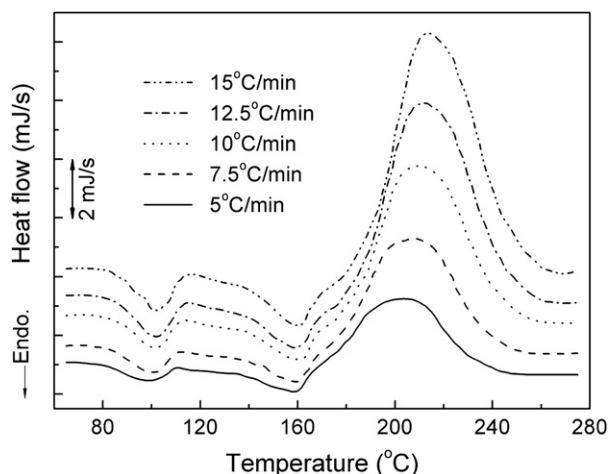


Fig. 7. DSC curves of BS-a dynamic polymerization at different heating rates.

Table 1

Peak temperatures and kinetic parameter values obtained from dynamic DSC scans.

Heating rate (°C/min)	T_p (°C)	Kissinger		Flynn–Wall–Ozawa
		E (kJ/mol)	A (s ⁻¹)	E (kJ/mol)
5	204.0	176.8	1.07×10^{16}	175.7
7.5	208.0			
10	211.0			
12.5	213.5			
15	215.5			

where C is a constant, T is the iso-conversion temperature, and the other parameters are the same as described previously. E can be obtained from the slope of the plot of $\ln\beta$ versus $1/T_p$.

According to the equations (2) and (3), the polymerization kinetic parameters were calculated and the results are listed in Table 1. It can be noticed that the activation energy values obtained by the two methods are very close.

In isothermal DSC mode, the polymerization reaction kinetics can be characterized by measuring the heat released during the reaction with temperature and time. It is assumed that the heat evolution recorded by DSC is proportional to the extent of consumption of the reactive groups. So, the extent of reaction (α) and the reaction rate ($d\alpha/dt$) during polymerization can be described as follows:

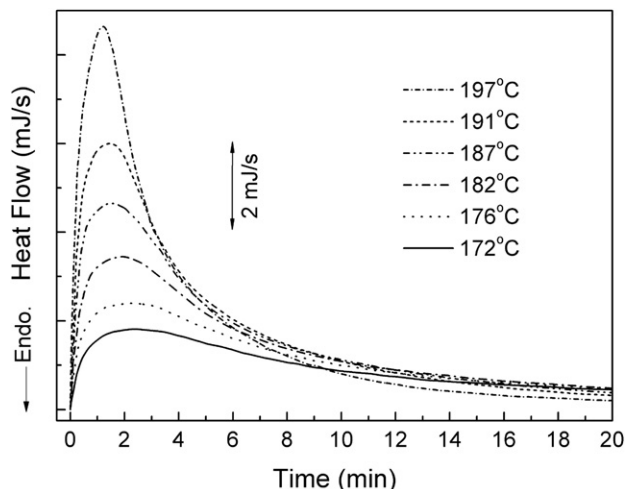


Fig. 8. DSC curves of BS-a isothermal polymerization at different temperatures.

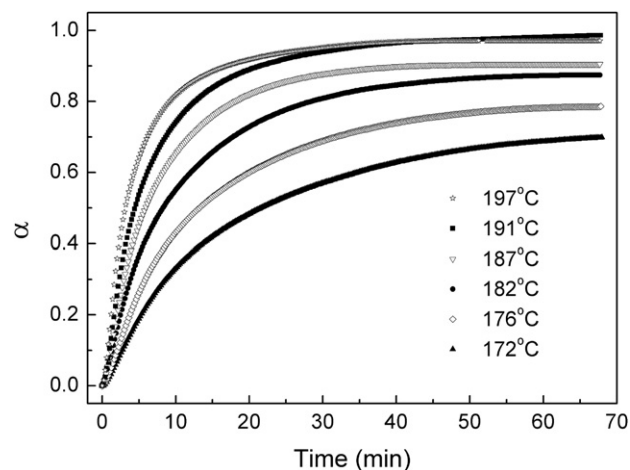


Fig. 9. Plots of conversion versus reaction time at different temperatures.

Table 2

Kinetic parameter values obtained from isothermal DSC scans.

Temperature (°C)	k (10 ⁻³ , s ⁻¹)	m	n	E (kJ mol ⁻¹)	A (s ⁻¹)
172	1.57	0.22	2.66	140.7	5.02×10^{13}
176	2.10	0.23	1.96		
182	3.50	0.30	2.01		
187	5.40	0.36	2.05		
191	7.38	0.41	1.87		
197	11.50	0.46	1.90		

$$\alpha = \frac{\Delta H_t}{\Delta H_0} \quad (4)$$

$$\frac{d\alpha}{dt} = \frac{1}{\Delta H_0} \times \frac{dH}{dt} \quad (5)$$

where ΔH_t is the reaction heat within time t , dH/dt is the flow rate of heat, and ΔH_0 is the total reaction heat, which is the maximum heat value determined among all the isothermal and dynamic polymerization reactions.

Fig. 8 shows the DSC curves of BS-a isothermal polymerization at different temperatures. It is clearly seen that the heat flow rate is a function of the polymerization temperature and time. The total exothermic reaction heat of BS-a is 305.3 J g⁻¹. According to

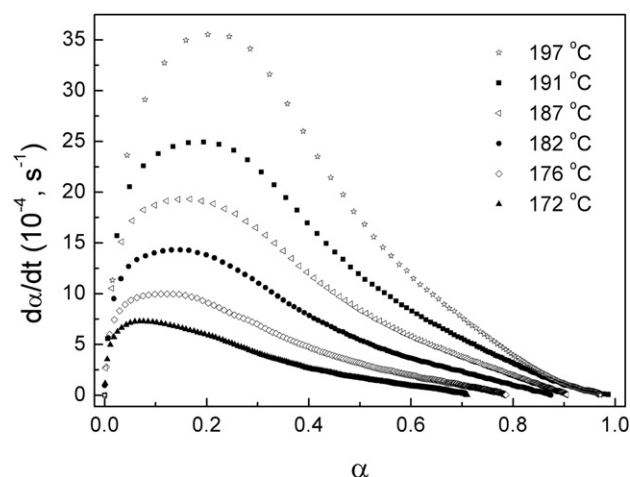


Fig. 10. Plots of reaction rate versus conversion at different temperatures.

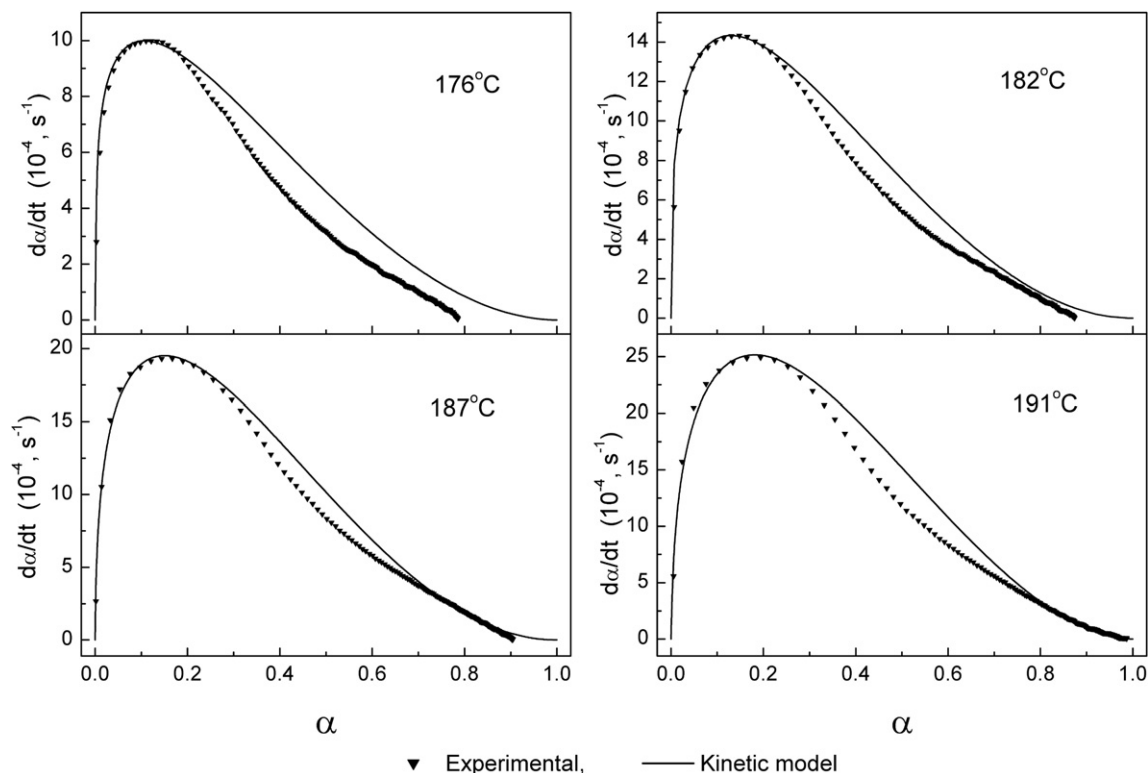


Fig. 11. Comparisons of the experimental results with the kinetic model data.

equations (4) and (5), α and $d\alpha/dt$ were calculated, and the plots of α versus t , $d\alpha/dt$ versus α at different temperatures are shown in Figs. 9 and 10, respectively.

The forgoing studies with FTIR show that the individual band conversion is affected by temperature and time. Also, it can be seen in Fig. 9 that the extent of the whole reaction process is affected by temperature and time. Here, it should be noted that the meanings of conversions given by FTIR and DSC methods are different, and the effects of temperature or time on conversions appear different. In FTIR, the conversions are obtained from the changes of absorption intensities of each selected group with an internal band as standard, while the conversions in DSC are obtained from the heat variation of all the reaction groups with the total exothermic reaction heat as quantitative standard. In addition, it can be noticed that the temperature ranges selected in the study are different for FTIR and DSC methods. In FTIR method, a relatively low temperature range was chosen to capture the small changes of the absorption intensities at a slow reaction rate. In DSC method, a relatively high temperature range was selected to determine sensitively the heat released during the reaction. Naturally, temperatures cannot be set too low or too high in DSC, at which the reaction heat cannot be measured effectively.

Fig. 10 shows that the reaction rate varied with the polymerization temperature and conversion, which phenomenologically shows the autocatalytic characteristics, and the reaction rate can be described by the following autocatalytic kinetic equation [50]:

$$\frac{d\alpha}{dt} = k\alpha^m(1-\alpha)^n \quad (6)$$

where m and n are the reaction orders, k is the rate constant at temperature T , following Arrhenius equation (7):

$$k = A \exp\left(-\frac{E}{RT}\right) \quad (7)$$

where all parameters have usual Arrhenius significance.

Based on the experimental data, kinetic parameters, k , m and n , can be obtained by fitting the experimental data to the equation (6) with nonlinear regression. Then, according to Arrhenius equation, activation energy (E) and pre-exponential factor (A) can be calculated via least squares linear regression. The results are listed in Table 2, and the comparisons of the experimental data with the kinetic model are shown in Fig. 11. The activation energy value is lower than the results obtained in dynamic mode.

In addition, comparing the kinetic results of BS-a with that of bisphenol-A based benzoxazine (BA-a) reported by Ishida and Rodriguez [19], it can be noticed that the activation energy values of BS-a are higher than that of BA-a. In the dynamic polymerization mode, the activation energy values of BS-a are 176.8 kJ/mol by Kissinger's method and 175.7 kJ/mol by Ozawa's method, respectively, while those of BA-a are 116 kJ/mol by Kissinger's method and 107 kJ/mol by Ozawa's method, respectively. In isothermal polymerization mode, the activation energy values of BS-a and BA-a are 140.7 kJ/mol and 102 kJ/mol, respectively. This may be ascribed to the structure difference between BS-a and BA-a monomers, namely, one is the rigid sulfone moiety – electron-withdrawing group, and the other is the flexible isopropyl – electron-donating group. In addition, it can also be noted that the reaction rate of BS-a is higher than that of BA-a at the same isothermal polymerization temperature. According to Arrhenius relationship (7), the reaction rate depends on the pre-exponential factor (A) and the activation energy (E) at the same temperature.

4. Conclusions

Bisphenol-S and aniline based benzoxazine monomer was synthesized with a solution method. The FTIR absorption

intensities of C–O–C, C–N–C, and oxazine ring decrease gradually with the temperature and time rising during the polymerization. The change rates of some absorption intensities of oxazine ring are affected by different atmosphere environments (air and nitrogen), and a higher degree of conversion is obtained in nitrogen than that in air at the same reaction temperature and in equal time. The polymerization reaction follows an autocatalytic mechanism.

References

- [1] Holly FW, Cope AC. *J Am Chem Soc* 1944;66:1875.
- [2] Ning X, Ishida H. *J Polym Sci Part A Polym Chem* 1994;32:1121.
- [3] Agag T, Jin L, Ishida H. *Polymer* 2009;50:5940.
- [4] Lin CH, Chang SL, Hsieh CW, Lee HH. *Polymer* 2008;49:1220.
- [5] Kim HJ, Brunovska Z, Ishida H. *Polymer* 1999;40:6565.
- [6] Santhosh Kumar KS, Reghunadhan Nair CP, Radhakrishnan TS, Ninan KN. *Eur Polym J* 2007;43:2504.
- [7] Andreu R, Espinosa MA, Galia M, Cadiz V, Ronda JC, Reina JA. *J Polym Sci Part A Polym Chem* 2006;44:1529.
- [8] Sponton M, Larrechi MS, Ronda JC, Galia M, Diz VC. *J Polym Sci Part A Polym Chem* 2008;46:7162.
- [9] Kiskan B, Koz B, Yagci Y. *J Polym Sci Part A Polym Chem* 2009;47:6955.
- [10] Ishida H, Ohba S. *Polymer* 2005;46:5588.
- [11] Agag T, Takeichi T. *Macromolecules* 2003;36:6010.
- [12] Hamerton I, Howlin BJ, Mitchell AL. *React Funct Polym* 2006;66:21.
- [13] Kim HJ, Brunovska Z, Ishida H. *J Appl Polym Sci* 1999;73:857.
- [14] Shen SB, Ishida H. *J Polym Sci Part B Polym Phys* 1999;37:3257.
- [15] Garea SA, Iovu H, Nicolescu A, Deleanu C. *Polym Test* 2007;26:162.
- [16] Kiskan B, Aydogan B, Yagci Y. *J Polym Sci Part A Polym Chem* 2009;47:804.
- [17] Jin L, Agag T, Ishida H. *Eur Polym J* 2010;46:354.
- [18] Ishida H, Heights S. US Patent. US5543516; 1996.
- [19] Ishida H, Rodriguez Y. *Polymer* 1995;36:3151.
- [20] Kim HJ, Brunovska Z, Ishida H. *Polymer* 1999;40:1815.
- [21] Kasapoglu F, Cianga I, Yagci Y, Takeichi T. *J Polym Sci Part A Polym Chem* 2003;41:3320.
- [22] Kumar S, Reghunadhan Nair CP, Ninan KN. *Thermochim Acta* 2006;441:150.
- [23] Chozhan CK, Alagar M, Gnanasundaram P. *Acta Mater* 2009;57:782.
- [24] Velez-Herrera P, Ishida H. *J Polym Sci Part A Polym Chem* 2009;47:5871.
- [25] Garea SA, Iovu H, Nicolescu A, Deleanu C. *Polym Test* 2009;28:338.
- [26] Santhosh Kumar KS, Reghunadhan Nair CP, Ninan KN. *Eur Polym J* 2009;45:494.
- [27] Takeichi T, Saito Y, Agag T, Muto H, Kawauchi T. *Polymer* 2008;49:1173.
- [28] Santhosh Kumar KS, Reghunadhan Nair CP, Sadhana R, Ninan KN. *Eur Polym J* 2007;43:5084.
- [29] Kiskan B, Demiray G, Yagci Y. *J Polym Sci Part A Polym Chem* 2008;46:3512.
- [30] Kiskan B, Yagci Y, Ishida H. *J Polym Sci Part A Polym Chem* 2008;46:414.
- [31] Cacal B, Cianga L, Agag T, Takeichi T, Yagci Y. *J Polym Sci Part A Polym Chem* 2007;45:2774.
- [32] Ning X, Ishida H. *J Polym Sci Part B Polym Phys* 1994;32:921.
- [33] Lin CH, Chang SL, Lee HH, Chang HC, Hwang KY, Tu PA, et al. *J Polym Sci Part A Polym Chem* 2008;46:4970.
- [34] Allen DJ, Ishida H. *J Appl Polym Sci* 2006;101:2798.
- [35] Macko JA, Ishida H. *Macromol Chem Phys* 2001;202:2351.
- [36] Dunkers J, Ishida H. *Spectrochim Acta Part A* 1995;51A:1061.
- [37] Allen DJ, Ishida H. *Polymer* 2009;50:613.
- [38] Allen DJ, Ishida H. *Polymer* 2007;48:6763.
- [39] Jin L, Agag T, Ishida H. *Eur Polym J* 2010;46:354.
- [40] Shen SB, Ishida H. *J Appl Polym Sci* 1996;61:1595.
- [41] Andreu R, Reina JA, Ronda JC. *J Polym Sci Part A Polym Chem* 2008;46:3353.
- [42] Rosu D, Cascaval CN, Mustata F, Ciobanu C. *Thermochim Acta* 2002;383:119.
- [43] Shi ZX, Yu DS, Wang YZ, Xu RW. *Eur Polym J* 2002;38:727.
- [44] Bartolomeo P, Chailan JF, Vernet JL. *Eur Polym J* 2001;37:659.
- [45] Russell VM, Koenig JL, Low HY, Ishida H. *J Appl Polym Sci* 1998;70:1413.
- [46] Yei DR, Fu HK, Chen WY, Chang FC. *J Polym Sci Part B Polym Phys* 2006;44:347.
- [47] Kissinger HE. *Anal Chem* 1957;29:1702.
- [48] Flynn JH, Wall LA. *Polym Sci Part B Polym Lett* 1966;4:323.
- [49] Ozawa T. *Bull Chem Soc Jpn* 1965;38:1881.
- [50] Kamal MR. *Polym Eng Sci* 1974;14:231.